



**HAL**  
open science

# Coupling the ISBA Land Surface Model and the TOPMODEL Hydrological Model for Mediterranean Flash-Flood Forecasting: Description, Calibration, and Validation

Ludovic Bouilloud, Katia Chancibault, Béatrice Vincendon, Véronique Ducrocq, Florence Habets, Georges-Marie Saulnier, Sandrine Anquetin, Eric Martin, Joël Noilhan

## ► To cite this version:

Ludovic Bouilloud, Katia Chancibault, Béatrice Vincendon, Véronique Ducrocq, Florence Habets, et al.. Coupling the ISBA Land Surface Model and the TOPMODEL Hydrological Model for Mediterranean Flash-Flood Forecasting: Description, Calibration, and Validation. *Journal of Hydrometeorology*, 2010, 2 (11), pp 315-333. 10.1175/2009JHM1163.1 . hal-00587936

**HAL Id: hal-00587936**

**<https://hal.science/hal-00587936>**

Submitted on 2 Nov 2021

**HAL** is a multi-disciplinary open access archive for the deposit and dissemination of scientific research documents, whether they are published or not. The documents may come from teaching and research institutions in France or abroad, or from public or private research centers.

L'archive ouverte pluridisciplinaire **HAL**, est destinée au dépôt et à la diffusion de documents scientifiques de niveau recherche, publiés ou non, émanant des établissements d'enseignement et de recherche français ou étrangers, des laboratoires publics ou privés.



Distributed under a Creative Commons Attribution 4.0 International License

## Coupling the ISBA Land Surface Model and the TOPMODEL Hydrological Model for Mediterranean Flash-Flood Forecasting: Description, Calibration, and Validation

LUDOVIC BOUILLOUD,<sup>\*,†,\*\*</sup> KATIA CHANCIBAULT,<sup>\*,#</sup> BÉATRICE VINCENDON,<sup>\*</sup>  
VÉRONIQUE DUCROCO,<sup>\*</sup> FLORENCE HABETS,<sup>@</sup> GEORGES-MARIE SAULNIER,<sup>&</sup>  
SANDRINE ANQUETIN,<sup>†</sup> ERIC MARTIN,<sup>\*</sup> AND JOEL NOILHAN<sup>\*</sup>

<sup>\*</sup> GAME/CNRM/Météo-France, CNRS, Toulouse, France

<sup>†</sup> CNRS/LTHE, Grenoble, France

<sup>#</sup> LCPC, Nantes, France

<sup>@</sup> CNRS/UMR SISYPHE, Paris, France

<sup>&</sup> CNRS/EDYTEM, Université de Savoie, Chambéry, France

(Manuscript received 19 February 2009, in final form 16 October 2009)

### ABSTRACT

Innovative coupling between the soil–vegetation–atmosphere transfer (SVAT) model Interactions between Soil, Biosphere, and Atmosphere (ISBA) and the hydrological model TOPMODEL has been specifically designed for flash-flood forecasting in the Mediterranean area. The coupled model described in this study combines the advantages of the two types of model: the accurate representation of water and energy transfer between the soil and the atmosphere within the SVAT column and an explicit representation of the lateral transfer of water over the hydrological catchment unit. Another advantage of this coupling is that the number of parameters to be calibrated is reduced by two, as only two parameters instead of four parameters concern the TOPMODEL formulation used here. The parameters to be calibrated concern only the water transfer. The model was calibrated for the simulation of flash-flood events on the three main watersheds covering the French Cévennes–Vivarais region using a subset of past flash-flood events having occurred since 2000. The complementary subset of flash-flood events was then used to carry out an objective verification of the coupled model after calibration. The evaluation on these six independent past flash-flood events shows satisfactory results. The comparison of the observed and simulated hydrographs demonstrates that no flash-flood peaks are missed. Relevant information for flash-flood forecasting can always be inferred from the simulations, even for those with quite poor results, making the system useful for real-time and operational flash-flood forecasting.

### 1. Introduction

The western Mediterranean region is regularly affected by devastating flash-flood events, particularly during autumn. These flash-floods have been responsible for human casualties and severe infrastructure damage. All the areas located close to the Mediterranean Sea are concerned by this phenomenon. In southern France, several extreme precipitation events associated with severe flash-

floods have occurred during recent decades (see Nuisser et al. 2008). This area is characterized by small-to-medium basins (with areas ranging from 10 to 1000 km<sup>2</sup>), with low baseflow rivers, sometimes intermittent, but possibly leading to very severe flash-floods during extreme precipitation events. For example, on 8–9 September 2002, a major convective system affected the Gard area in the Cévennes–Vivarais region (Fig. 1). A comprehensive description of this hydrometeorological event can be found in Delrieu et al. (2005) and Ducrocoq et al. (2008). This event was particularly remarkable for its spatial extent, with rain amounts greater than 200 mm in 24 hours over 5500 km<sup>2</sup>. The maximum value reached 600–700 mm in places. The observed peak discharge of the rivers was very high, more than twice the 10-yr return period discharge of the region. For example, the peak discharge of

<sup>\*\*</sup> Current affiliation: Météo-France, Toulouse, France.

Corresponding author address: Ludovic Bouilloud, Météo-France, DPREVI/GCRI, 42 Avenue Gaspard Coriolis, 31057 Toulouse CEDEX, France.  
E-mail: ludovic.bouilloud@meteo.fr

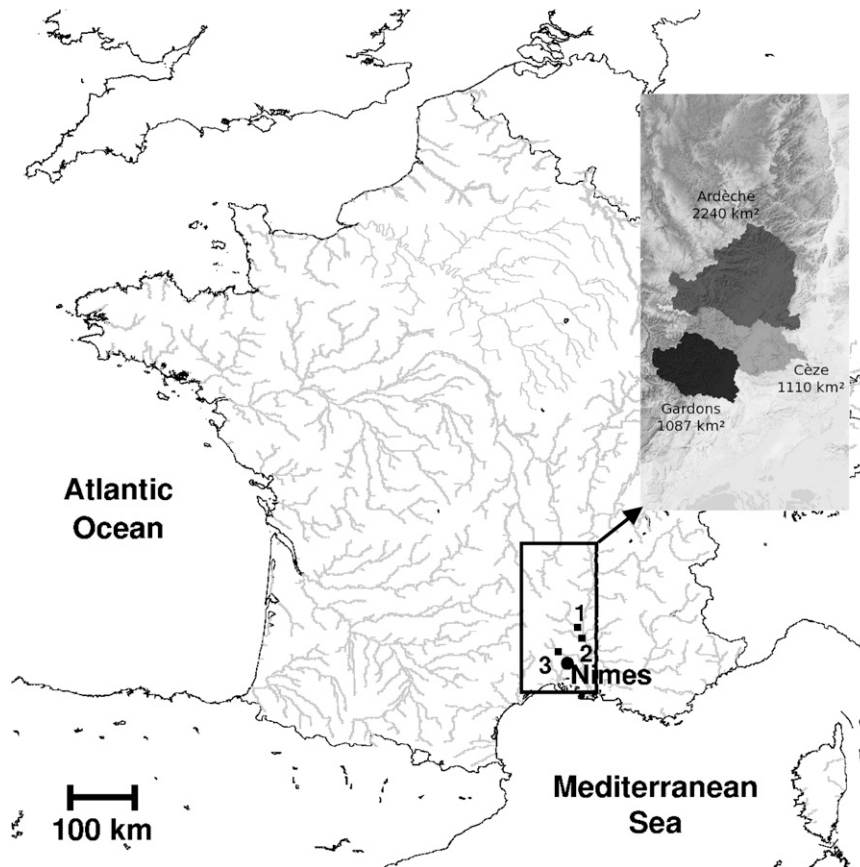


FIG. 1. Location of the Cévennes–Vivarais region within France and location of outlets of the Ardèche River (1 = Saint-Martin), the Cèze River (2 = Bagnols/Cèze), and the Gardons River (3 = Boucoiran). The upper window shows the corresponding three watersheds. The gray lines represent the hydrographic network.

the Gard River basin ( $1700 \text{ km}^2$ ) was estimated as greater than  $6000 \text{ m}^3 \text{ s}^{-1}$ . This event was responsible for 24 human deaths and economic damage estimated at €1.2 billion (Huet et al. 2003).

The hydrological response of the catchments in this region is mainly controlled by subsurface flows and fast runoff generation on contributing areas (Lardet and Obled 1994; Taha et al. 1997). During the lateral redistribution of rainfall infiltration within the subsurface of a hillslope, soil saturation can occur where the local topographic/pedological/geomorphological properties of the soil show little capacity for lateral transfer of the water and/or where the preexisting soil moisture deficit is smallest. These locations are called contributing areas because rainfall cannot infiltrate any more as a result of the water saturation of the subsurface soil. This leads to quick surface runoff generated by a saturation excess (Cappus 1960; Dune and Black 1970). Lateral redistribution of subsurface soil water content is therefore a major hydrological process to be taken into

consideration in flash-flood simulation. The hydrological model TOPMODEL (Beven and Kirkby 1979; Beven et al. 1995) was one of the first attempts to model distributed hydrological responses based on the variable contributing area concept. The original TOPMODEL model and some of its derived versions have been shown to simulate realistic discharge for the Cévennes–Vivarais watersheds (Pellenq et al. 2003; Pellarin et al. 2002; Saulnier and Datin 2004; Le Lay and Saulnier 2007), showing that the underlying concepts of TOPMODEL are relevant for these catchment areas.

Besides the space–time structure of the rainfall, Le Lay and Saulnier (2007) pointed out the importance of the initial soil water content on the accuracy of the simulated flash-flood hydrograph. Contrary to what was generally believed for extreme heavy rainfall events, they found, for the extreme event that occurred in September 2002 in the Gard region, that not only the rainfall but also the initial water content controlled the flash-flood event. A way to account for initial soil conditions in hydrological

models is to couple the hydrological model with a soil–vegetation–atmosphere transfer (SVAT) model. An important deficiency in soil–vegetation–atmosphere transfer models is the lack of explicit processing for spatial horizontal variability in soil moisture redistribution. So, the coupling of a SVAT model with a hydrological model permits advantages to be drawn from each modeling principle—that is, an explicit representation of water and heat transfer within the soil column and a representation of the lateral water transfer to determine the horizontal distribution of the soil moisture.

Coupling SVATs with hydrological models is not new (Famiglietti et al. 1992; Famiglietti and Wood 1994; Stieglitz et al. 1997; Ducharme et al. 2000; Chen and Kumar 2001; Pellenq et al. 2003; Niu and Yang 2003), but it is generally applied on the global or regional scale. The coupling presented in this paper is designed for a different context. It is conceived for simulation at the fine time scale of a flash-flood event and for medium hydrological watersheds (order of 1000 km<sup>2</sup>). It is a combination of the land surface model Interactions between Soil, Biosphere, and Atmosphere (ISBA; Noilhan and Planton 1989; Noilhan and Mahfouf 1996) and the hydrological model TOPMODEL (Beven and Kirkby 1979; Beven et al. 1995). Unlike in previous works coupling ISBA and TOPMODEL (Habets and Saulnier 2001; Pellenq 2002; Decharme and Douville 2006), the TOPMODEL concepts are applied to the watershed unit here and not as a one-dimensional parameterization independently operating on each SVAT grid column. This allows the lateral water transfer to be computed by considering the watershed as a physical unit defined at 50-m resolution rather than introducing a subgrid-scale parameterization of it for each individual ISBA 1-km grid mesh. Furthermore, compared with previous couplings with ISBA, this version of TOPMODEL takes advantage of the dynamic drainage area calculation detailed in Pellarin et al. (2002) and of the analytical solving of a bias in the catchment area water balance (Saulnier and Datin 2004). This ISBA–TOPMODEL system was developed and evaluated in the framework of the prevention, information, and early warning (PREVIEW) European Commission's Sixth Framework Programme (FP6) Integrated Project. The aim of this project was the development of real-time operational flash-flood forecasting systems for Mediterranean watersheds using high-resolution hydrometeorological coupled systems (Vincendon et al. 2008). The specific aim of this paper is, after a calibration step inherent in all hydrological models, to describe the advanced ISBA–TOPMODEL coupled system and to show its capabilities on several flash-flood events that occurred over the watersheds of the Cévennes–Vivarais region. A companion study

(Vincendon et al. 2009, manuscript submitted to *J. Hydrol.*) evaluates the benefit of coupling ISBA with TOPMODEL for soil moisture distribution and discharge simulation.

Following this introduction, section 2 describes the principles of the ISBA–TOPMODEL system. A more comprehensive description of the coupled system is provided in appendix. Section 3 presents the calibration of the coupled system we ran on five past flash-flood events and examines the sensitivity of the coupled system to the time–space rainfall used to drive the system. Then, section 4 discusses the results of the evaluation of the model on six additional flash-flood events. Our conclusions are presented in section 5.

## 2. Description of ISBA/TOPMODEL

Figure 2 presents a schematic view of the coupled system based on the ISBA land surface model and the TOPMODEL hydrological model. Appendix provides a detailed description of the coupled system; only the main concepts of each model and the coupling are presented in this section.

### a. ISBA land surface model

The ISBA land surface model simulates the interaction between the soil, the biosphere, and the atmosphere and forms part of Météo-France's numerical weather prediction, research, and climate atmospheric models Action de Recherche Petite Echelle Grande Echelle (ARPEGE; Courtier and Geleyn 1988), ALADIN (Bubnová et al. 1993), mesoscale nonhydrostatic (MESO-NH; Lafore et al. 1998), and Applications of Research to Operations at Mesoscale (AROME; Seity et al. 2008). ISBA is a physically based scheme that solves the water and energy budgets. It is a one-dimensional model and, consequently, only vertical transfer is considered. In the present study, ISBA was run on a 1-km<sup>2</sup> Lambert conformal grid over a rectangular domain, including the three main watersheds of the Cévennes–Vivarais region (Fig. 1). This fine horizontal resolution was selected to facilitate the use of radar rainfall products or of the new generation of high-resolution numerical weather models, such as the Météo-France AROME model.

The ISBA version used in this study was the 3-layer version based on the force–restore method (Deardorff 1977). It calculates the time evolution of the surface and mean soil temperatures, the water interception storage reservoir, and the three soil moisture and ice buckets (Noilhan and Mahfouf 1996; Boone et al. 2000). In the original version of ISBA, a subgrid runoff  $R$  was introduced (Habets et al. 1999), based on the Variable Infiltration Capacity (VIC) principle described in Wood

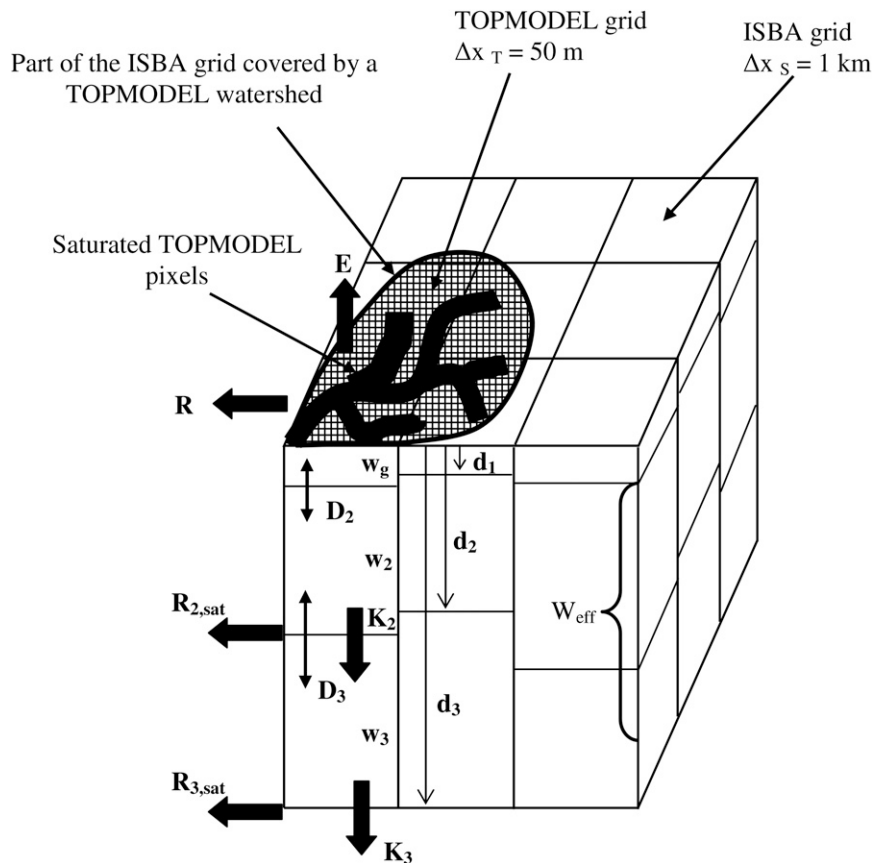


FIG. 2. Schematic view of the coupling between ISBA and TOPMODEL. The ISBA and TOPMODEL horizontal mesh are represented by  $\Delta x_S$  and  $\Delta x_T$ , respectively;  $d_1$ ,  $d_2$ , and  $d_3$  are the depths of the bare soil layer, the root-zone layer, and the subroot zone layer, respectively; diffusion is represented by  $D$ ; gravitational drainage is represented by  $K$ ; the mean volumetric water content of each layer is given by  $w$ ; runoff is represented by  $R$ ; evapotranspiration is denoted by  $E$ ; and  $W_{\text{eff}}$  represents the effective water content available for lateral transfer.

et al. (1992) and Dümenil and Todini (1992). This is different in the coupled system, in which runoff is estimated using the saturated area contribution following TOPMODEL principles. To be consistent with the TOPMODEL assumptions (Beven 1982), we also used a saturated hydraulic conductivity  $k_{\text{sat}}$  in ISBA, which followed an exponential decrease with soil depth (Chen and Kumar 2001; Decharme et al. 2006; Quintana Seguí et al. 2008b):

$$k_{\text{sat}}(z) = k_{\text{sat},c} e^{-f(z-d_c)}, \quad (1)$$

where  $z$  (m) is the depth,  $f$  ( $\text{m}^{-1}$ ) is the exponential decay factor, and  $d_c$  (m) is the compacted depth. The compacted depth is defined as the depth at which vertical water motion is made difficult by the compacted soil. Above the compacted depth, roots and organic matter favor the development of macropores and facilitate water movement. This formalism assumes that,

at the depth  $d_c$ , the saturated conductivity reaches the compacted value  $k_{\text{sat},c}$  given by Clapp and Hornberger (1978).

#### b. TOPMODEL hydrological model

TOPMODEL has been increasing in popularity since it was first proposed, because it provides a relatively simple framework for the use of digital terrain model data and computationally efficient prediction of distributed hydrological responses. TOPMODEL makes use of a topographic index of hydrological similarity based on an analysis of the topographic data. For this study, the digital elevation model (DEM) was defined at 50-m resolution.

Among the several versions of TOPMODEL, we selected one well suited to the hydrological context of Mediterranean catchments (Saulnier et al. 1998). The main modifications introduced in this version allowed better conservation of mass (Saulnier and Datin 2004;

Habets and Saulnier 2001) and also took the rainfall spatial variability into account through a dynamic hydrological index (Pellarin et al. 2002),

$$\lambda_{i,t} = \ln\left(\frac{a_{i,t} r_{i,t}}{\tan\beta_i}\right), \quad (2)$$

where  $a_{i,t}$  (m) is the total upslope area draining in pixel  $i$ , per unit contour length;  $\tan\beta_i$  is the local topographic slope, and  $r_{i,t}$  ( $\text{m s}^{-1}$ ) is the hillslope recharge of the water table, which depends of the rainfall spatial and temporal distribution. The hydrological index allows the hydrological behavior of a pixel to be represented. The upslope draining area characterizes the pixel ability to collect upstream water, and the local topographic slope characterizes its ability to evacuate downstream water. For example, a pixel located close to the river, with a high draining area and a low slope, will have a high index, representative of a low evacuation ability and a high saturation capacity. In contrast, a pixel located on a crest, with a low draining area and a high slope, will have a low index representative of its low saturation ability.

The local storage deficit  $d_{i,t}$  is then determined as follows:

$$d_{i,t} = M(\bar{\lambda} - \lambda_{i,t}) + \bar{d}_t, \quad (3)$$

where  $\bar{\lambda}$  and  $\bar{d}_t$  are the mean hydrological index and the mean storage deficit, respectively, over the catchment. Here  $M$  is the rate of decrease of transmissivity with depth and may be linked to the effective depth  $\Delta z_{\text{eff}}$  (see appendix) or active storage of the catchment soil profile. The pixels for which the local deficit is predicted as zero ( $d_{i,t} = 0$ ) constitute the saturated contributing areas.

### c. Coupling

The coupling between ISBA and TOPMODEL was performed as follows. As in previous applications of TOPMODEL over the Cévennes–Vivarais watersheds, the lateral distribution with TOPMODEL was performed each hour. So, at each TOPMODEL time step, the hillslope recharge and the storage deficit were updated from the ISBA water content of the soil layer of depth  $\Delta z_{\text{eff}}$ . Then TOPMODEL performed the lateral distribution of water over the catchment according to Eq. (3) and predicted the saturated contributing areas. The saturated areas and the new water content were then aggregated on the ISBA mesh, and the surface runoff was computed by ISBA. It also computed the deep drainage and subsurface saturation excess runoff. The total runoff and drainage at each ISBA mesh were then routed at the TOPMODEL time step frequency to the outlet using a geomorphological

method (Le Lay et al. 2008). As in most hydrological models, some parameters relative to the water transfer within the soil needed to be calibrated in the coupled system. These were the effective depth for lateral water distribution  $\Delta z_{\text{eff}}$  and the parameters relative to the exponential profile of saturated hydraulic conductivity, that is, the decay factor  $f$  and the compacted depth  $d_c$ . We assumed that the effective depth and the compacted depth had the same value, which reduced to two the number of parameters to be calibrated. It is physically acceptable to consider that the depth below the surface where most of the vertical transfers occur is close to that where horizontal transfer is active.

## 3. Model calibration

### a. Experimental setup

The calibration of the coupled model followed a standard procedure. The parameter values were sought by comparing the hydrograph obtained by repeated simulations with the observed discharge for a given catchment. These calibration methods were needed to define, before their application, the size of the parameter space, the incremental step for spanning the parameter space, and a statistical score measuring the accuracy of the simulated hydrograph versus the measured one. Also, a reliable dataset of observations (accurate rainfall field and discharge measurement) was needed, which is not straightforward, to obtain for intense flash-flood events. One aim of the Cévennes–Vivarais Mediterranean Hydrometeorological Observatory (Delrieu et al. 2005) is precisely to improve the observation of the Mediterranean intense rain events and associated devastating flash floods for model calibration and validation. This effort started in 2000 and currently comprises two weather radars, about 400 daily rain gauges and 160 hourly rain gauges, and about 45 water level stations within a  $160 \times 200 \text{ km}^2$  area centered over the Cévennes–Vivarais region. This high-density observation network provided the high-resolution data necessary to calibrate and validate our model. Actually, the high density of rain gauges enabled accurate 1-h accumulated rainfall fields to be established with a kriging method (Lebel et al. 1987) for the highly precipitating events of recent years. The observed discharges for the three main watersheds of the domain—the Gardons, the Ardèche, and the Cèze Rivers—were also used. However, because of the frequent breakdown of the water level station at the main outlet of the Gardons River, simulations were completed for a secondary outlet located at Boucoiran. The outlets associated with the Ardèche and the Cèze Rivers are the Saint-Martin and Bagnols/Cèze, respectively.

The watershed areas are 1087 km<sup>2</sup> for the Gardons, 1110 km<sup>2</sup> for the Cèze, and 2240 km<sup>2</sup> for the Ardèche. The location of the catchments and their associated outlets are given in Fig. 1.

The initial conditions for the simulation (soil water and temperature profiles) were taken from the Météo-France hydrometeorological operational system, SAFRAN-ISBA coupled model (MODCOU; Habets et al. 2008) running at 8 km. The other meteorological parameters needed to drive the ISBA model also came from this system, more specifically from the SAFRAN analysis [see Quintana Seguí et al. (2008a) for a comprehensive description of the system]. It includes the 2-m temperature and humidity, the 10-m wind speed, the surface pressure, and the short- and longwave radiation. All the 8-km resolution data were interpolated on the 1-km ISBA grid of the coupled system. The simulations started two days before the start of the heavy precipitation events, allowing the soil water conditions to be balanced before the event. This 2-day spin-up delay was deduced from a test of sensitivity carried out for two heavy rain events. The first event occurred from 5 to 9 September 2005 (corresponding to event D in Table 1); for this event, the initial soil moisture was quite low. The second event, from 29 November to 3 December 2003, was a part of the event 5 (see Table 5 below). So the rainy events that occurred before the 29 November 2003 led to relatively high initial soil moisture. For each event, two simulations were performed. The first one (simulation 1 in Fig. 3) started a few hours before the identified rain event (at 0000 UTC), whereas the second one (simulation 2 in Fig. 3) started 48 hours sooner. The results are illustrated for one watershed (Gardons for the September 2005 event and Ardèche for the December 2003 event) in Fig. 3. For both events, the simulated discharge during the observed flood was approximately the same for both simulations. However, for the event with wet initial conditions, a delay of approximately 48 hours after the start of the simulations is necessary to reach the soil moisture balance. The 48-h spin-up delay was therefore considered to be long enough to properly simulate flash floods. The calibration and validation excluded this 48-h spin-up period.

### b. Calibration of the model

As described in section 2, two parameters needed to be calibrated:  $f$  and  $d_c$  of the saturated hydraulic conductivity profile. These parameters are very important because they determine the vertical distribution of soil moisture and therefore the surface runoff and the deep drainage. In the following, the compacted depth is expressed as a function of the root depth ( $d_2$ ) following the relation  $d_c = \alpha d_2$ . So, the aim of the calibration was to

TABLE 1. List of flash-flood events used for the ISBA-TOPMODEL system calibration for the three watersheds, where RR is the mean cumulated rainfall within the catchment (mm) and  $Q_{\max}$  is the maximum discharge observed at the outlet (m<sup>3</sup> s<sup>-1</sup>).

| Event | Date of simulation | Gardons |            | Cèze |            | Ardèche |            |
|-------|--------------------|---------|------------|------|------------|---------|------------|
|       |                    | RR      | $Q_{\max}$ | RR   | $Q_{\max}$ | RR      | $Q_{\max}$ |
| A     | 14–22 Oct 2001     | 195     | 687        | 119  | 728        | 183     | 1443       |
| B     | 5–12 Sep 2002      | 343     | 6699       | 271  | 2994       | 125     | 1320       |
| C     | 31 Oct–7 Nov 2004  | 63      | 336        | 84   | 475        | 108     | 1379       |
| D     | 3–11 Sep 2005      | 285     | 436        | 247  | 469        | 204     | 444        |

obtain an optimized value of  $\alpha$  and  $f$  for each catchment. To do this, we performed a large number of simulations on several flash-flood events spanning the possible parameter space. As a first guess for these parameters, we took the values found by Decharme et al. (2006) for the Rhône basin:  $f = 2.68 \text{ m}^{-1}$  and  $\alpha = 1$ . Because the rivers considered in our study are tributaries of the Rhône, these values constituted a reasonable guess. Then, for the variation range around these values, we considered values proposed in the literature. The decay factor can vary widely. For example, Famiglietti et al. (1992) proposed a range from 1.5 to 5.17 m<sup>-1</sup>, and Stieglitz et al. (1997), Niu and Yang (2003), and Chen and Kumar (2001) proposed 3.26, 4, and 1.8 m<sup>-1</sup>, respectively. We chose to vary  $f$  from 1 to 4 by 1 m<sup>-1</sup> steps and  $\alpha$  from 0.25 to 1.5, by steps of 0.25, to stay close to the values given in Decharme et al. (2006) for the same region with the ISBA model. These 24 simulations were performed on each of the past flash-flood events listed in Table 1. Although the calibration was performed on a limited number of these events, the sample contained quite different hydrological events. Besides the exceptional flash-flood case of September 2002 (event B), three more classical cases were selected. Moreover, unlike the other events, which were composed of a single flow peak, event D contained two flow peaks, the second peak being enhanced by saturated soils from the first rainy episode.

As a measure of goodness of fit to the hydrograph, the Nash efficiency quadratic score (Nash and Stutcliffe 1970) was used:

$$\text{Nash} = 1 - \frac{\sum_{i=1}^N (Q_{\text{sim},i} - Q_{\text{obs},i})^2}{\sum_{i=1}^N (Q_{\text{obs},i} - \overline{Q_{\text{obs}}})^2}, \quad (4)$$

where  $Q_{\text{sim},i}$  is the simulated discharge,  $Q_{\text{obs},i}$  is the observed discharge, and  $\overline{Q_{\text{obs}}}$  is the mean observed discharge. This score is frequently used in hydrological model calibration. Moreover, this statistic gives important weight to high discharge values, so it is well suited to our context

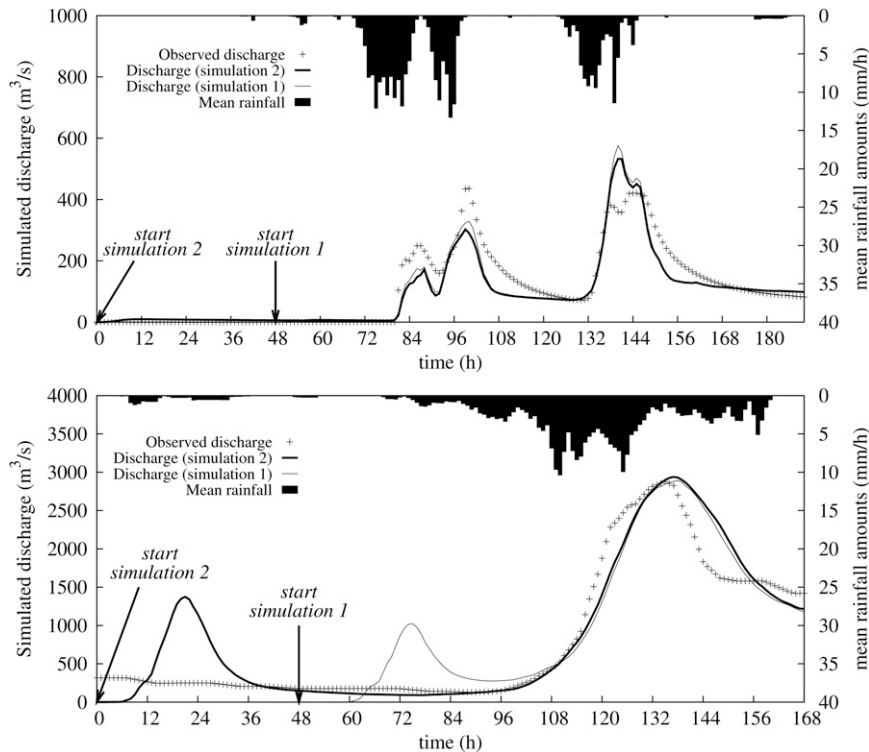


FIG. 3. (top) Sensitivity test of a 48-h spinup for a dry soil initial condition for the Gardons watershed and (bottom) a wet soil initial condition for the Ardèche watershed.

of simulating intense events and forecasting their peak discharge. The aim of the calibration was to determine the parameters leading to a Nash efficiency as close as possible to the value 1 (perfect agreement). Regarding the size of the time window around the flash-flood event on which the Nash efficiency is computed, Reed et al. (2004) showed that it had little effect on their conclusions. For each simulation, scores were therefore calculated for a time window starting from day 2 of the simulation to its end.

Figure 4 shows the Nash efficiency values computed for each set of simulations over each catchment area and for each event. For a majority of events and watersheds, a pair of coefficients that allowed a satisfactory simulation of the discharge (i.e., with a Nash efficiency greater than 0.7) was found. However, the parameter pairs leading to the best results could vary according to the event. This was particularly true for the Gardons and Cèze Rivers. Pairs that led to satisfactory results for one event could lead to very poor results for another event. For example, concerning the Cèze River for event B, the best results were obtained with high values of  $\alpha$  (greater than or equal to 1), whereas these values led to poor results for event D. For the Ardèche River, it can be noted from Fig. 4 that the best results were obtained with approximately the same parameter values whatever the

event. On the basis of the best Nash efficiency averaged over the four events, a pair of parameters was selected for each watershed (Table 2). The effective depth on which the lateral transfer was performed by TOPMODEL was therefore equal to the ISBA root layer for the Gardons and Ardèche watersheds, whereas it was only 75% of the root layer depth for the Cèze watershed. The  $f$  parameter values selected were rather high, between 3 and 4  $\text{m}^{-1}$ . These results were, however, in agreement with the calibration study completed at the scale of France as a whole for the SAFRAN-ISBA-MODCOU operational suite (Quintana Seguí et al. 2008b), with high values of the  $f$  parameter (greater than 3  $\text{m}^{-1}$ ) for the watersheds considered. In contrast, the results for the  $\alpha$  parameter were quite different. In our study, we found larger values of these parameters [0.75 or 1 versus 0.25 for the study by Quintana Seguí et al. (2008b)]. This might be due to the slightly different meaning of  $\alpha$ . With the ISBA-TOPMODEL coupled model described here, this parameter is not only a parameterization of the vertical water transfer but it also represents the effective depth for lateral transfer.

### c. Results of simulations with the calibrated model

To consolidate our choice of calibrated parameter values, the simulated discharge using these parameters

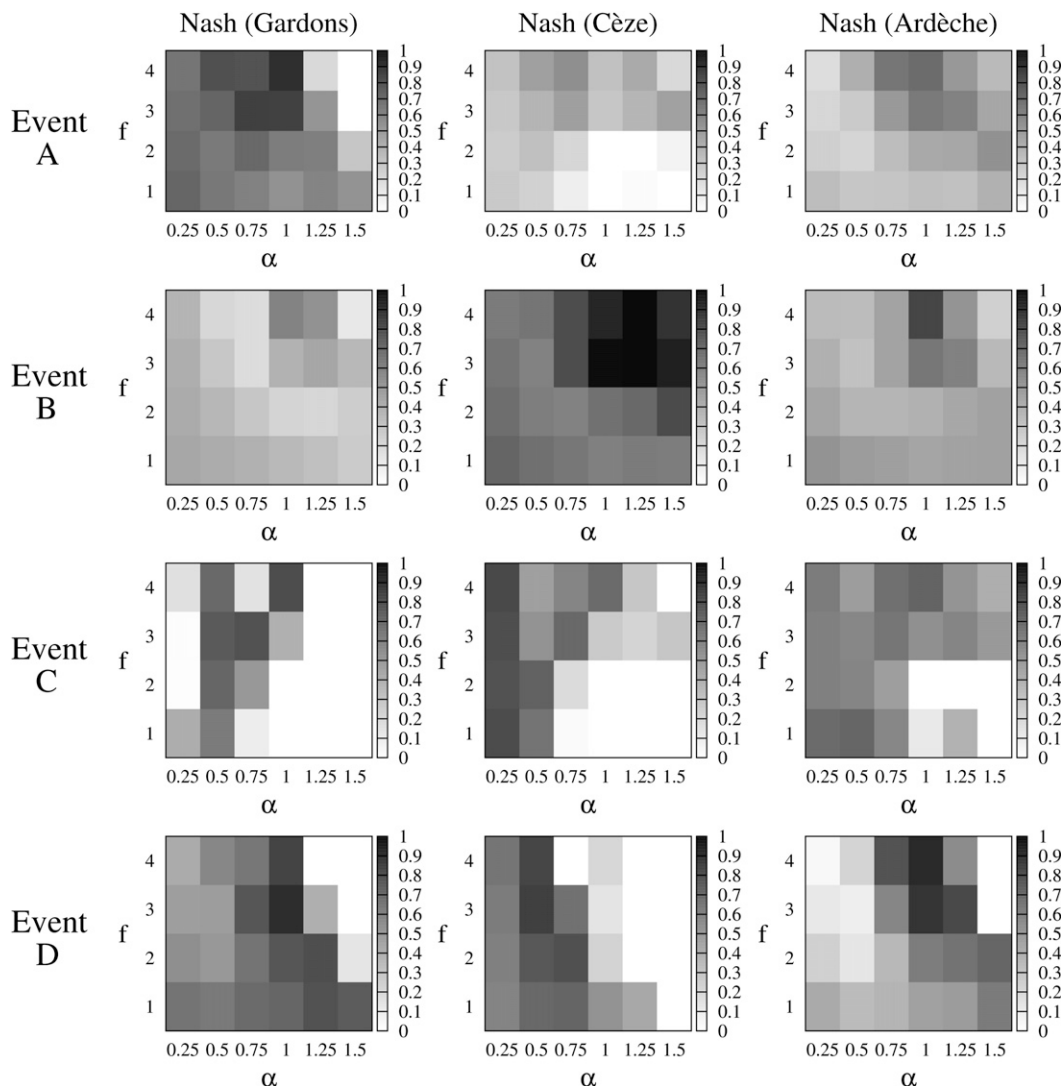


FIG. 4. Nash efficiency for the four events (A–D in Table 1) used for calibration for the three watersheds considered and for each  $(\alpha, f)$  pair.

was systematically compared with the observed hydrograph for the three watersheds and the four events. Table 3 gives a set of statistical scores obtained for each event simulation using the coupled model once calibrated. The scores computed were the Nash efficiency, the relative error in discharge volume (REDV), and the relative error in maximum discharge (REMD). For the relative scores, a negative (positive) value means that the model underestimates (overestimates) the discharge. Results varied among events and watersheds. However, for most cases, the Nash efficiency was close to or greater than 0.7, which was quite satisfactory. Figure 5 shows the simulated and observed discharge time series for event D, which occurred from 3 to 11 September 2005 with a peculiar timing. During this event, the major peak, which

induced casualties, happened during the second rainfall episode even though it was associated with a lower amount of rainfall. The discharge was simulated by the ISBA–TOPMODEL system with relatively good accuracy for the three watersheds. Despite some discrepancies on the flow peak amplitudes, the flood dynamics were relatively well simulated. These results were confirmed by

TABLE 2. Calibrated  $f$  and  $\alpha$  parameters for the Gardons, Cèze, and Ardèche watersheds.

| Watershed | $f$ | $\alpha$ |
|-----------|-----|----------|
| Gardons   | 4   | 1        |
| Cèze      | 3   | 0.75     |
| Ardèche   | 4   | 1        |

TABLE 3. Scores [Nash, REDV (%), and REMD (%)] for the simulations on the Gardons, Cèze and Ardèche watersheds for calibration events A–D.

| Event | Gardons |       |       | Cèze |       |       | Ardèche |       |       |
|-------|---------|-------|-------|------|-------|-------|---------|-------|-------|
|       | Nash    | REDV  | REMD  | Nash | REDV  | REMD  | Nash    | REDV  | REMD  |
| A     | 0.87    | 11.5  | −18.3 | 0.45 | 19.5  | −64.3 | 0.66    | −20.7 | −37.1 |
| B     | 0.57    | −12.7 | −38.8 | 0.78 | −14.0 | −42.0 | 0.80    | −9.2  | −26.9 |
| C     | 0.78    | 19.3  | −5.6  | 0.68 | 31.1  | −6.8  | 0.69    | 11.8  | −9.7  |
| D     | 0.81    | −14.4 | 22.2  | 0.65 | 60.2  | 13.5  | 0.89    | −7.3  | −18.9 |

quite good scores obtained for the Gardons and Ardèche watersheds (Nash efficiencies of 0.81 and 0.89, respectively). For the Cèze watershed, statistical results were less satisfactory. As can be seen in Fig. 5, the weak scores can be attributed to a failure of the model to represent the beginning of the event correctly. The increase of the simulated flood occurred several hours before the measured one. However, the second peak was quite accurately simulated.

For the exceptional case of September 2002 (event B), the discharge in the observed database associated with this event was much higher than in other events for the Gardons and Cèze watersheds (a maximum of approximately  $6700 \text{ m}^3 \text{ s}^{-1}$  for the Gardons watershed). For these catchments, results showed an underestimation of the maximum discharge of about 40%. The simulated discharge reached  $4100 \text{ m}^3 \text{ s}^{-1}$  for the Gardons watershed, which was lower than the observed flow peak. But this was a very high flow peak for this watershed compared with the other simulated peaks. Thus, relevant information concerning the flood risk was, nevertheless, obtained thanks to this simulation. Because the hourly rainfall and discharge related to this event were very high, great uncertainties were associated with the measurements, which could explain a part of the discrepancies between the observed and simulated hydrographs. Bonnifait et al. (2009) showed that the rating curves (transformation of the measured water height into discharge) were highly uncertain for extreme events. In particular, they showed that the maximum observed discharge of this event and watershed may have been significantly overestimated. Another possible cause of discrepancy could be the model parameterization. The model was calibrated with less extreme events, so the parameters may have been unsuitable for such exceptional values. Note that, for the Ardèche River, which experienced weaker rainfall and discharges for this event, the simulation quality was better than for the other two watersheds. Because the additional perspective of the model is a real-time forecasting application, the main quality expected from such a system is more to be able to forecast the risk of a high discharge rather than to provide a precise hydrograph. Consequently, these discrepancies are not prohibitive

and we can conclude that the simulation performed with the calibrated model did rather well in highlighting this risk of flash flooding.

#### d. Sensitivity to rainfall fields

The high sensitivity of the TOPMODEL hydrological model to time–space rainfall distribution has already been shown (Zehe et al. 2005; Le Lay and Saulnier 2007). In our coupled system, TOPMODEL discharge is not yet directly driven by the rainfall but by the water content simulated by ISBA. To see if the sensitivity of the discharge simulation to the input rainfall was still high, some sensitivity tests were carried out using various types of rainfall fields. In addition to the hourly kriged rainfall, two other kinds of precipitation were considered: precipitation from the SAFRAN analysis (Quintana Seguí et al. 2008a) and precipitation derived from radars. The objective of the SAFRAN analysis is to produce the most accurate estimation of the atmospheric variables and downward fluxes needed to force the ISBA model. SAFRAN uses an optimal interpolation method to analyze the parameters (Gandin 1963). The analysis is performed over climatically irregular homogeneous zones and then interpolated on a regular  $8 \times 8 \text{ km}^2$  regular grid. The precipitation rate is estimated daily using the high-resolution daily rain gauge network (3500 stations in France) and then disaggregated at an hourly time step, based on the evolution of the relative humidity of the air (precipitation is constrained to occur when the relative humidity is high). The partition between snowfall and rainfall is based on the  $0.5^\circ\text{C}$  limit. The radar data come from the Météo-France operational weather radar located in Nîmes (see Fig. 1 for location). These data were corrected using a monthly multiplicative factor. The sensitivity tests were performed for event D using the calibrated version of ISBA–TOPMODEL. This event was selected first because of its interesting timing with two successive intense rainfall episodes of the same intensity leading to two different hydrological responses. Other reasons for choosing this case were that the event was well simulated by the coupled system for the Gardons watershed (Nash = 0.81) and that radar data were available for this

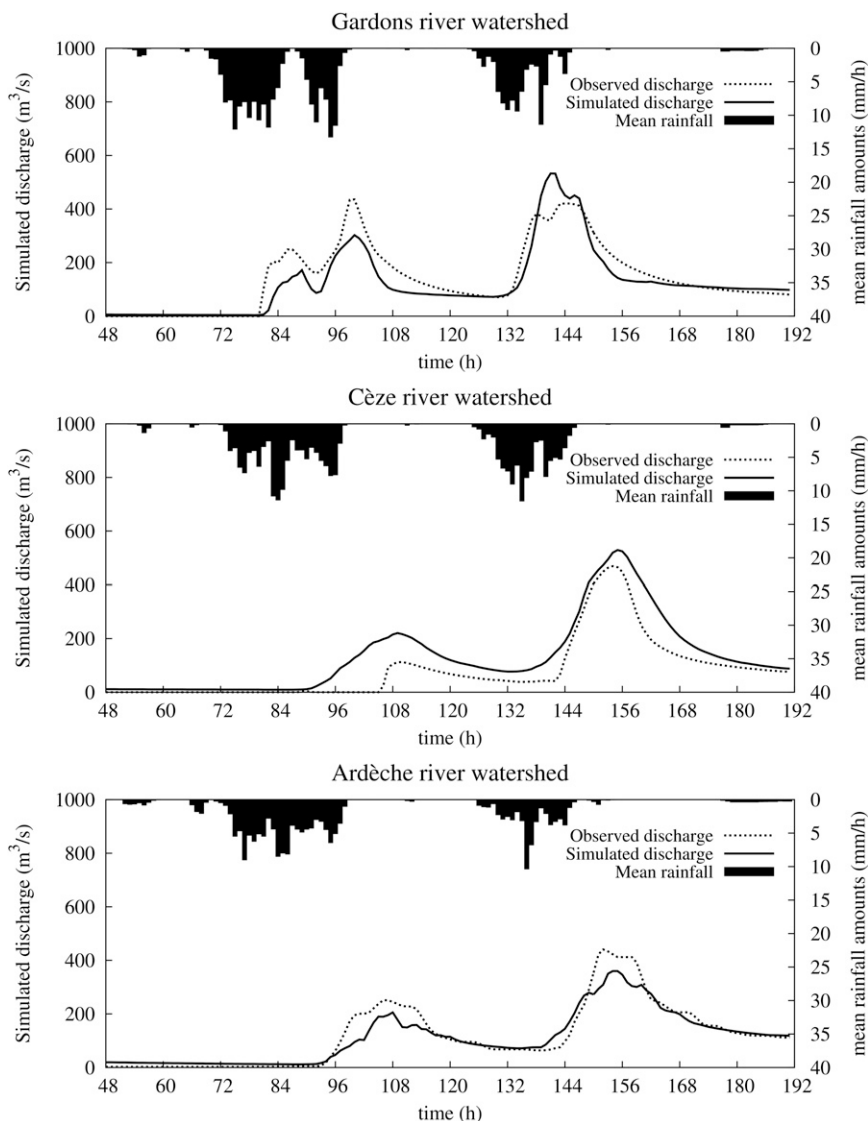


FIG. 5. Comparison of observed and simulated discharge for the flash-flood event period from 5 to 11 Sep 2005 (event D) and for the Gardons, Cèze, and Ardèche River watersheds.

case. Figure 6 shows the simulated discharge using the kriged, SAFRAN, and radar precipitation compared to the observed hydrograph for the Gardons watershed. Results were quite similar for the two other catchments. Using SAFRAN or radar rainfall led to a significant worsening of the quality of the simulated hydrograph compared to kriged rainfall. These results were confirmed by Nash efficiencies of only 0.45 and 0.37 for the SAFRAN and radar rainfall, respectively (Table 4). The simulation using radar data clearly underestimated the discharge because of an underestimation of the rainfall amount by the radar. Actually, for the radar data, the mean accumulated rainfall was 249 mm, whereas for the kriged rainfall it was 285 mm. The timing of the two flow

peaks was, however, almost preserved. This was not the case for the simulation using the SAFRAN rainfall, in which the dynamics of the discharge was reproduced with poor accuracy (Fig. 6). This was due to an already identified failure of the SAFRAN analysis for estimating the convective precipitation in the Cévennes region (Quintana Seguí et al. 2008a). Unlike the other meteorological variables, the SAFRAN analysis uses the daily precipitation observations, and the hypotheses used for disaggregating them at a hourly time step are no longer valid where convective precipitation is concerned.

To further analyze the sensitivity to the rainfall field, some additional experiments were carried out using the kriged rainfall averaged in time or in space. In a first

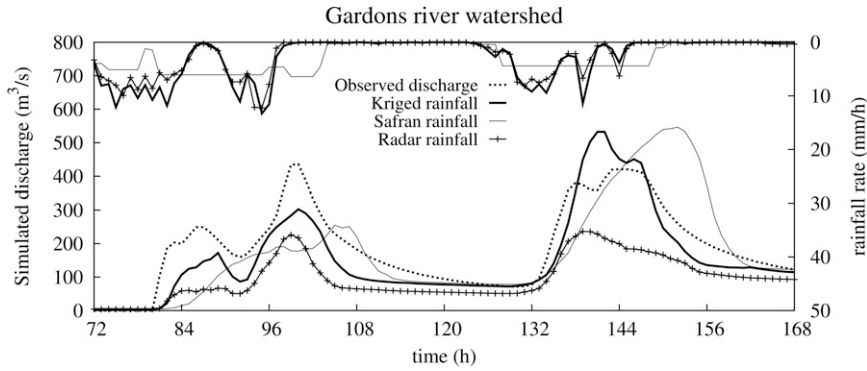


FIG. 6. Comparison of observed discharge with simulated discharge using kriged, SAFRAN, and radar precipitation input for the flash-flood event period from 3 to 12 Sep 2002 (event B) and for the Gardons River watershed.

experiment, the rainfall was averaged in space over the catchment. The statistics for this experiment were not as good as for the experiment using the original kriged field (Table 4). Although the flow dynamics remained approximately the same as the original kriged field, the peaks were lowered (Fig. 7). Then, in a second set of experiments, the hourly kriged rainfall was averaged in time, over 3-, 6-, and 12-h sliding time windows. The 3-, 6-, and 12-h accumulation was then equally distributed over each hour. Scores show significant differences between using the 12-h averaged rainfall and the 3- or 6-h average rainfall fields. When the 12-h averaged rainfall was used, the simulation was noticeably deteriorated. The discharge dynamics was not well simulated and was comparable to the one obtained with the SAFRAN rainfall (Fig. 6). These results confirmed that a large accumulated period for rainfall was not able to capture the rapid time evolution of the heavy precipitation event and therefore the evolution of the flash-flooding event. Concerning the simulation completed with a 6-h time step, results were close to those obtained with the hourly time step rainfall in terms of scores. However, relative discrepancies existed in the simulation of the discharge with the 6-h time step (Fig. 7) in comparison with the hourly kriged rainfall simulation. The simulation with the 3-h averaged rainfall was quite similar to the one with the hourly kriged rainfall. So, considering the hourly kriged rainfall as reference, it can be concluded that 3-h accumulated rainfall is acceptable for a possible operational use, whereas accumulating rainfall beyond six hours is insufficient. The tests described in this section confirm that the sensitivity to the input rainfall field, in terms of both spatial and temporal distribution, is still high when the coupled system is used.

**4. Model evaluation**

To evaluate the robustness of the calibration of the coupled system performed in section 3, the system was

evaluated on an independent sample of flash-flood events (Table 5). Besides “ordinary” flash-flood events, a 23-day-long event made up of a succession of three flash-flood events was also simulated (event 5).

The Nash efficiency, the relative error in discharge volume, and the relative error in maximum discharge for the six events and for the three watersheds are given in Table 6. More than half of the watersheds and events have Nash efficiency values larger than 0.7. As expected, the results of simulations for the evaluation events are poorer than those obtained in the calibration phase. The mean Nash efficiency (computed for all the watersheds and events) was approximately 0.6 for the validation, whereas it reached 0.7 for the calibration. As in section 3c, the majority of poor simulations show an underestimation of the discharge but all simulate a flood (i.e., the overflowing of the river). The simulation of event 6 gave particularly good scores whichever the watershed (Table 6). The comparison of the simulated hydrographs with those observed (Fig. 8) confirms the results of the scores.

The visual inspection of some simulated hydrographs shows that the recession phase lasts longer in simulation than in observations. This phenomenon can be noted for

TABLE 4. Mean error ( $m^3 s^{-1}$ ) and Nash efficiency for simulations using different types of rainfall input: hourly kriged, SAFRAN rainfall, radar rainfall, mean spatially averaged hourly rainfall, and 3-, 6- or 12-h averaged kriged rainfall.

| Precipitation type                        | Mean error | Nash |
|---|------------|------|
| Kriged (hourly)                           | -21.0      | 0.81 |
| SAFRAN                                    | -8.4       | 0.45 |
| Radar                                     | -65.9      | 0.37 |
| Kriged but averaged on the catchment      | -42.2      | 0.66 |
| Kriged but averaged with a 3-h time step  | -22.2      | 0.80 |
| Kriged but averaged with a 6-h time step  | -25.2      | 0.80 |
| Kriged but averaged with a 12-h time step | -26.1      | 0.72 |

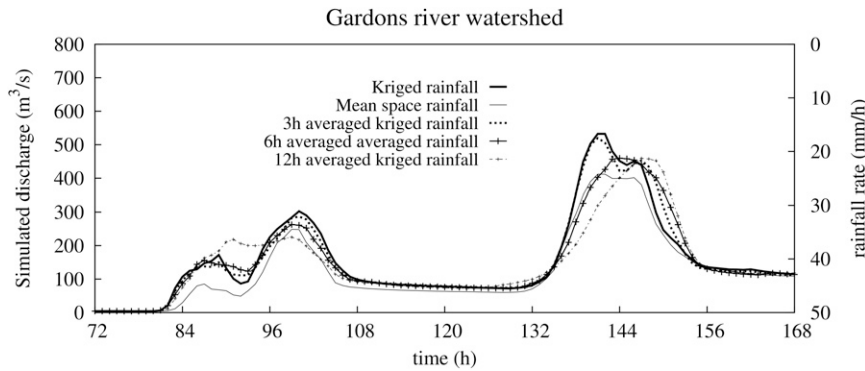


FIG. 7. Comparison of simulated discharge for the flash-flood event period from 3 to 12 Sep 2002 (event B) and for the Gardons River watershed using kriged rainfall, with simulation using mean kriged rainfall on the catchment and averaging over several time steps (3, 6, 12 h) of the kriged rainfall.

event 3 for the Cèze and the Ardèche watersheds, with Nash efficiency values of  $-0.13$  and  $0.01$ , respectively. The simulated and observed hydrographs are shown for the Cèze watershed in Fig. 9. The simulated flow peak fits the observed one quite well, but the simulated recession is very slow compared to the observation. Moreover, the base flow of the river, before the event, is largely overestimated in the simulation, and it might be due to the poor quality of the initial conditions extracted from the SAFRAN-ISBA-MODCOU operational system. These two reasons lead to weak statistics. The same conclusion can be drawn for the Ardèche watershed. As far as events 2 and 4 are concerned, the simulations did not perform very well for some watersheds, with a Nash efficiency lower than  $0.6$ . As for event 3, the baseflow discharge was overestimated in the simulation, except for the Ardèche watershed. In contrast, the simulated dynamics were satisfactory even if the maximum discharge was underestimated. These differences in baseflow discharge or recession phase are, however, not critical for the forecasting of flash flooding. So, in most cases, the simulation is satisfactory, and even when it is not, relevant information concerning the flood risk is still provided. Finally, we found no major difference between the results for calibration and the independent

events. Therefore, we can conclude that the calibration of the model is quite robust.

Another point of interest was the behavior of the model in a long-term (with respect to the flash-flood scale) simulation. This simulation corresponds to event 5. For this event, which contained three flash floods in a 23-day period, the Nash efficiency was found to be satisfactory for the three watersheds,  $0.63$ ,  $0.77$ , and  $0.87$  for the Gardons, Cèze, and Ardèche River watersheds, respectively. The simulated and observed hydrographs are presented in Fig. 10 for the three watersheds. First of all, no bias appeared when the model was run for a long time, with a quite accurate baseflow interevent simulation. The dynamics of the three flash floods was, moreover, accurately simulated for each watershed. In particular, the three events started at the same moment in simulations and observations for most cases, although some discrepancies existed in the timing of the peak discharge (except for the Cèze watershed). This may be seen as an objective advantage of this coupling compared to event-based flash-flood hydrological models. This coupling ensures a better representation of interstorm hydrological processes (evaporation, transpiration, vertical transfers) and obviates the need for a reinitialization of soil water contents at the beginning of a storm,

TABLE 5. Same as Table 1 but for the ISBA-TOPMODEL system evaluation for the three watersheds.

| Event | Date of simulation | Gardons |                  | Cèze |            | Ardèche |            |
|-------|--------------------|---------|------------------|------|------------|---------|------------|
|       |                    | RR      | $Q_{\max}$       | RR   | $Q_{\max}$ | RR      | $Q_{\max}$ |
| 1     | 24 Sep–2 Oct 2000  | 166     | 893              | 101  | 236        | 129     | 1024       |
| 2     | 7–18 Nov 2000      | 129     | 402              | 85   | 379        | 143     | 1720       |
| 3     | 1–10 Oct 2001      | 109     | 202              | 118  | 428        | 74      | 902        |
| 4     | 18–30 Nov 2002     | 124     | Sensor breakdown | 103  | 469        | 157     | 1480       |
| 5     | 11 Nov–6 Dec 2003  | 587     | 1314             | 422  | 892        | 532     | 2970       |
| 6     | 21–31 Oct 2004     | 173     | 452              | 164  | 442        | 218     | 2010       |

TABLE 6. Same as Table 3 but for events 1–6.

| Event | Gardons |         |         | Cèze  |       |       | Ardèche |       |       |
|-------|---------|---------|---------|-------|-------|-------|---------|-------|-------|
|       | Nash    | REDV    | REMD    | Nash  | REDV  | REMD  | Nash    | REDV  | REMD  |
| 1     | 0.69    | 41.5    | -48.0   | 0.82  | 39.0  | -13.1 | 0.69    | -26.0 | -42.8 |
| 2     | 0.23    | 99.5    | 73.4    | 0.57  | 28.4  | -27.9 | 0.70    | -19.3 | -34.6 |
| 3     | 0.72    | 76.0    | -20.8   | -0.13 | 167.1 | 4.4   | 0.01    | 83.5  | 28.1  |
| 4     | No data | No data | No data | 0.55  | -19.5 | -31.8 | 0.41    | -34.8 | -26.0 |
| 5     | 0.63    | 20.5    | 30.4    | 0.77  | 15.6  | 36.7  | 0.87    | -4.5  | 14.0  |
| 6     | 0.85    | -14.7   | -31.0   | 0.9   | 24.7  | -6.7  | 0.80    | -10.7 | -27.6 |

unlike event-based flash-flood hydrological models. The first two flashfloods were slightly underestimated, whereas the third flash flood, which was the largest one, was a little overestimated. For the Ardèche River, which

experienced the largest observed discharge, the maximum observed discharge for the third flash flood was approximately  $2970 \text{ m}^3 \text{ s}^{-1}$ , whereas the simulated discharges reached  $3350 \text{ m}^3 \text{ s}^{-1}$ . So, this last flash flood,

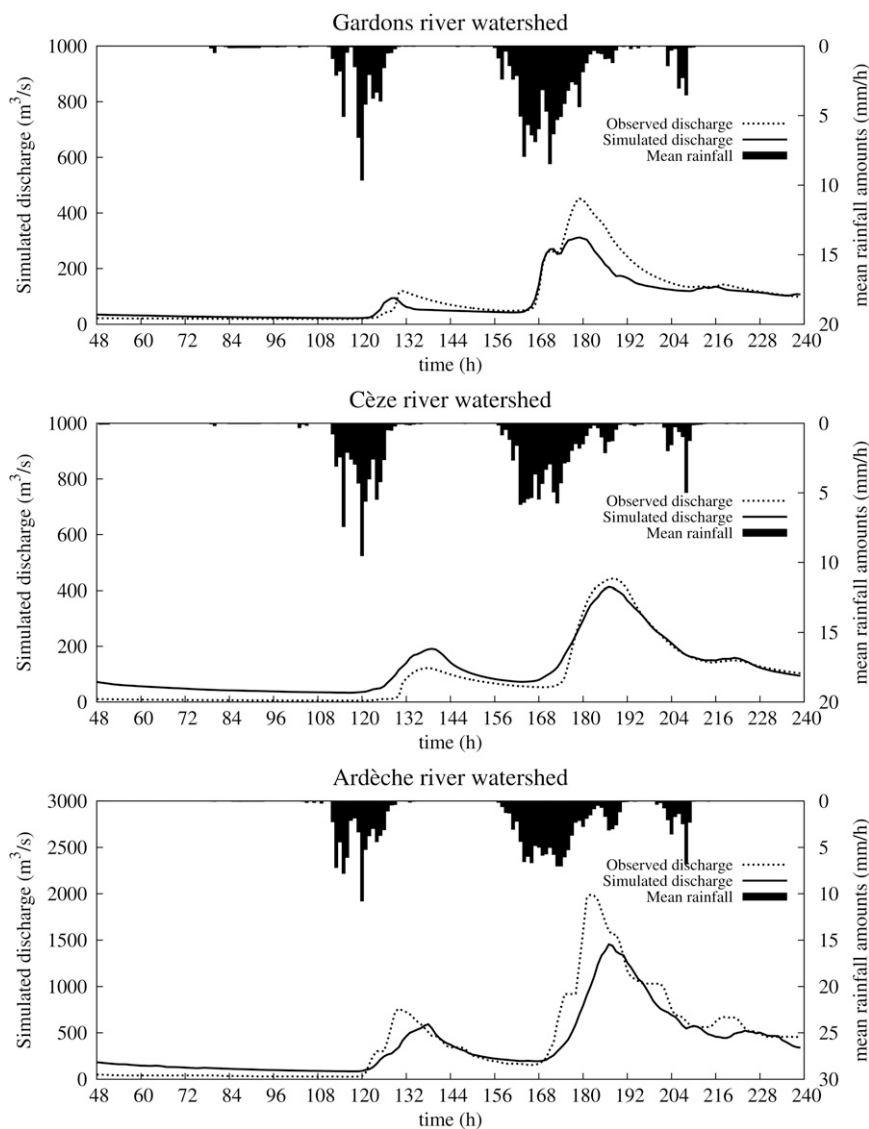


FIG. 8. Comparison of observed and simulated discharge for the flash-flood event period from 21 to 31 Oct 2004 (event 6) and for the Gardons, Cèze, and Ardèche River watersheds.

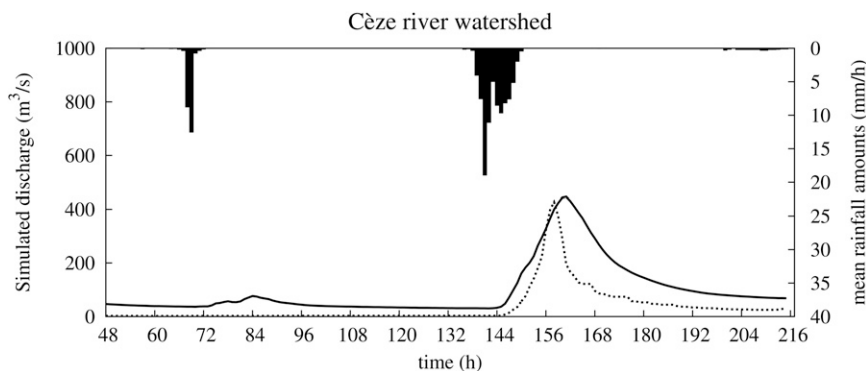


FIG. 9. Same as Fig. 8 but for the period from 1 to 10 Oct 2001 (event 3) for the Cèze watershed.

which was an extreme event, was simulated with appreciable accuracy, as also indicated by the Nash efficiency obtained for this event and watershed (Table 6). Thus, as pointed out for other events of the evaluation database, the differences (peak timing, peak discharge underestimation) are not critical for flash-flood forecasting. However, the timing simulation might be improved in future works, following progress in the representation of water transfer in the soil, at the surface, and in the river, instead of the simplified representation used in this study. Moreover, this study did not focus on timing accuracy, so the speed parameter sensitivity tests (appendix) were completed only for one event. So, the use of the model for purposes of accurate hydrological representation of phenomena will need particular effort concerning the calibration of these parameters.

## 5. Conclusions and discussion

Coupling between the SVAT model ISBA and the hydrological model TOPMODEL has been designed. This coupled model allows the advantages of the two types of models to be combined: the accurate representation of water and energy transfer between the soil and the atmosphere within the SVAT column and an explicit representation of the lateral transfer of water over the hydrological catchment unit. With this coupling, we go one step further than previous studies in the way the TOPMODEL concepts are introduced in a SVAT model. The lateral distribution of water is not conceived as a surface runoff subgrid-scale parameterization operating within the individual SVAT soil columns using statistical distribution of the topographic similarity index over the SVAT rectangular grid (Habets et al. 1999; Decharme et al. 2006). Instead, the lateral water transfer and the contributing areas are evaluated considering the watershed as a physical unit and with a topographic similarity index explicitly defined using a 50-m resolution

digital elevation model. In a companion study based on idealized simulations, Vincendon et al. (2009, manuscript submitted to *J. Hydrol.*) have shown that the surface runoff and the soil water content produced by the ISBA–TOPMODEL coupled system are more physically consistent than those produced by ISBA alone.

One advantage of the ISBA–TOPMODEL system compared to the original TOPMODEL hydrological model is that the number of parameters to be calibrated is reduced by two. The two parameters to be calibrated concern the water transfer in the soil. The model was therefore calibrated for the simulation of flash-flood events on three watersheds located in the French Cévennes–Vivarais region and associated with the Gardons, Cèze, and Ardèche Rivers. The Cévennes–Vivarais Mediterranean Hydrometeorological Observatory, started in 2000, provided the observations of flash-flood events required for the calibration and evaluation of the coupled system. Ten events that have occurred since 2000 were separated into two samples: one for calibration and the other for independent evaluation. Even though the size of the sample for the calibration seemed a little low, it was possible to determine a pair of calibrated parameters that led to a reasonable simulation of the hydrograph for the 10 events. This calibration procedure might be improved in the future with the increasing number of extreme events in the database. At this stage, the simulations completed with the calibrated model permit us to conclude that the calibration is quite robust and that it enables satisfactory simulation of the peak flow.

Among the events selected for the evaluation, one covered a long period compared to the flash-flood time scale. It lasted approximately one month and comprised a succession of three flash floods. Applying the ISBA–TOPMODEL system over the entire period and not over the individual events allowed us to show the robustness of the system, with no bias generated. Moreover, the system succeeded in capturing the three successive

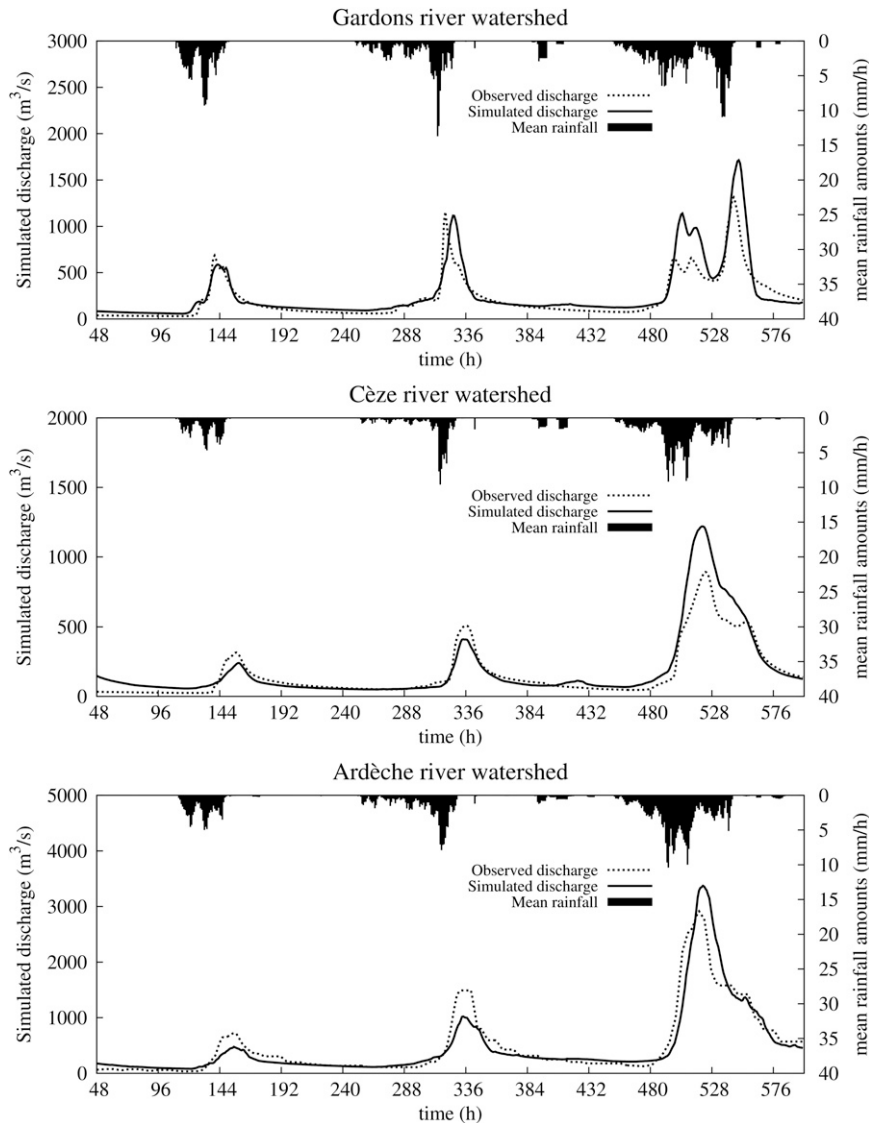


FIG. 10. Same as Fig. 8 but for the period from 11 Nov to 3 Dec 2003 (event 5) and for the Gardons, Cèze, and Ardèche River watersheds.

flash floods well. Regarding the other events, statistics indicated variable quality according to the event and the watershed. However, the visual inspection of the observed and simulated hydrographs when the statistics were poor showed that relevant information for the flash-flood forecasting could nevertheless be inferred. These results enable the system to be considered for real-time flash-flood forecasting. The first results using high-resolution numerical weather rainfall forecast instead of kriged rainfall observations are encouraging (Vincendon et al. 2008), even though the quality of the forecast discharge is highly dependent on the uncertainties of the rainfall forecast.

One other advantage of this coupling is that, technically, the ISBA model is already coupled with Météo-France's

atmospheric models, so the coupling of the ISBA–TOPMODEL system with the atmospheric models is easily conceivable. In the future, this will allow a study of the feedbacks to the atmosphere of improved soil water content produced by the ISBA–TOPMODEL coupling.

## APPENDIX

### Description of the Coupled System

#### *a. ISBA soil water content prognostic equations*

The governing equations of ISBA for the time evolution of soil moisture for the three soil layers are written as

$$\frac{\partial w_g}{\partial t} = \frac{C_1}{\rho_w d_1} (I - E_g) - D_1 \quad (\text{A1})$$

$$\frac{\partial w_2}{\partial t} = \frac{1}{\rho_w d_2} (I - E_g - E_{tr}) - K_2 - D_2, \quad \text{and} \quad (\text{A2})$$

$$\frac{\partial w_3}{\partial t} = \frac{d_2}{d_3 - d_2} (K_2 + D_2) - K_3, \quad (\text{A3})$$

where  $K$  ( $\text{s}^{-1}$ ) is the gravitational drainage of soil water,  $D$  ( $\text{s}^{-1}$ ) is the vertical soil moisture diffusion, and  $C_1$  is a dimensionless force–restore coefficient. The density of liquid water is  $\rho_w$  ( $\text{kg m}^{-3}$ ), the superficial soil depth is  $d_1$  (m), the depth of the rooting layer is  $d_2$  (m), and the total soil depth is  $d_3$  (m; Fig. 2). This depth can be considered to be reached when soil moisture changes with respect to time can be neglected.

In Eqs. (A1) and (A2), bare soil evaporation and plant transpiration rates ( $\text{m s}^{-1}$ ) are represented by  $E_g$  and  $E_{tr}$  (Noilhan and Mahfouf 1996), respectively; plant transpiration continues, whereas the root zone water content is larger than the wilting point volumetric water content  $w_{\text{wilt}}$ . The infiltration rate  $I$  is given by

$$I = P_g - R, \quad (\text{A4})$$

where  $P_g$  is the rate of precipitation reaching the surface and  $R$  is the surface runoff.

### b. Soil hydrological parameters

The soil hydrological parameters and the force–restore coefficients are related to the soil texture properties and moisture using expressions from Clapp and Hornberger (1978). Soil texture properties are taken from the National Institute of Agronomical Research (INRA) 1-km soil geographical database [Base de Données Géographique des Sols de France (BDGSF), available online at [www.gissol.fr/programme/bdgsf/bdgsf.php](http://www.gissol.fr/programme/bdgsf/bdgsf.php)]. Only the percentages of sand and clay are used to define the soil parameters for ISBA (Noilhan and Lacarrere 1995). The soil depth and the surface cover are derived from the ECOCLIMAP database (Masson et al. 2003); 215 ecosystems representing areas of homogeneous vegetation are derived by combining existing land cover maps and climate maps, in addition to using Advanced Very High Resolution Radiometer (AVHRR) satellite data. The very fine resolution of the data (1 km) over the globe allows for the initialization of the surface parameters of the models down to the 1-km scale. This database permits the initializing of the force–restore parameters, the soil hydrological parameters, and the saturated hydraulic conductivity  $k_{\text{sat},c}$  ( $\text{m s}^{-1}$ ) at the compacted depth. In the ISBA model, soil textures—and consequently the derived

parameters—are considered to be vertically homogeneous. The saturated hydraulic conductivity is, however, allowed to vary vertically, using the exponential profile [see Eq. (3) in section 2] introduced into the ISBA model by Decharme et al. (2006) following the formalism of Chen and Kumar (2001). The TOPMODEL mean watershed exponential rate of decrease  $M$  is linked to  $f$  as follows:

$$M = \frac{1}{n} \sum_n \frac{w_{\text{sat}} - w_{\text{fc}}}{f}, \quad (\text{A5})$$

where  $n$  is the number of ISBA meshes within the catchment,  $w_{\text{sat}}$  ( $\text{m}^3 \text{m}^{-3}$ ) is the effective porosity (or water content at saturation), and  $w_{\text{fc}}$  is the field capacity ( $\text{m}^3 \text{m}^{-3}$ ). The effective porosity is the porosity accounting for the presence of ice within the soil.

### c. Lateral water transfer

The lateral water distribution is determined within each TOPMODEL catchment by considering that the active layer for the lateral water transfer has a depth  $\Delta z_{\text{eff}}$ . First, the water content  $w_{\text{eff}}$  of this layer over the ISBA grid is estimated as the depth-weighted average of the water contents  $w_2$  and  $w_3$ . Then,  $w_{\text{eff}}$  is disaggregated on each TOPMODEL pixel to estimate the hillslope recharge of the water table  $r_{i,t}$  in Eq. (2) of section 2. So, the water recharge of a TOPMODEL pixel  $i$  within an ISBA mesh  $I$  is given by

$$r_{i,t} = \max[0, \min(w_{i,t}, w_{\text{sat}}) - w_{\text{fc}}] \Delta z_{\text{eff}}. \quad (\text{A6})$$

The water content  $w_{i,t}$  of TOPMODEL pixel  $i$  is determined by the time variation of  $w_{\text{eff}}$  over mesh  $I$  during one TOPMODEL time step  $\delta t$  (i.e.,  $\delta t = 1$  h):

$$w_{i,t} = w_{i,t-\delta t} + (w_{\text{eff},I,t} - w_{\text{eff},I,t-\delta t}). \quad (\text{A7})$$

If a TOPMODEL pixel is already saturated, then the water above saturation is disseminated among the other nonsaturated pixels of the ISBA mesh.

Next, the mean storage deficit  $\bar{d}_I$  over the watershed is evaluated from the water table and the maximum local deficit  $d_{\text{max}}$  at each pixel  $i$  is

$$d_I = \sum_i (d_{\text{max}} - r_{i,t}) \quad \text{and} \quad (\text{A8})$$

$$d_{\text{max}} = \max[w_{\text{sat}} - \min(w_{i,t}, w_{\text{fc}})] \Delta z_{\text{eff}}. \quad (\text{A9})$$

Water is redistributed over the watershed according to Eq. (3) of section 2, assuming the conservation of the mean storage deficit. Equation (3) thus provides the local storage deficit  $d_{i,t}$  after the lateral transfer of water and

updates the water content at each TOPMODEL pixel. Averaging the water content values over each TOPMODEL pixel within the ISBA mesh allows the ISBA water contents to be updated.

#### d. Runoff and drainage production

In the ISBA–TOPMODEL coupled system, the surface runoff production over an ISBA mesh is estimated through the saturated areas computed by TOPMODEL over the watershed:

$$R = P \frac{a_{\text{sat}}}{a_{\text{ISBA}}}, \quad (\text{A10})$$

where  $a_{\text{sat}}$  is the area of contributing saturated TOPMODEL pixels within the given ISBA mesh.

The subsurface runoffs  $R_{2,\text{sat}}$  and  $R_{3,\text{sat}}$  (Fig. 2) that are produced when the water content of the rooting layer and of the total soil exceed the saturation level are added to the surface runoff. They are given by

$$R_{2,\text{sat}} = \frac{\rho_w d_2}{\Delta t} \max[0, (w_2 - w_{\text{sat}})] \quad \text{and} \quad (\text{A11})$$

$$R_{3,\text{sat}} = \frac{\rho_w (d_3 - d_2)}{\Delta t} \max[0, (w_3 - w_{\text{sat}})], \quad (\text{A12})$$

where  $\Delta t$  is the ISBA time step.

The total deep drainage at the bottom of the soil column also follows the original ISBA formulation

$$\rho_w (d_3 - d_2) K_3 = \rho_w d_3 \frac{C_3}{\tau} \max[0, (w_3 - w_{\text{fc}})], \quad (\text{A13})$$

where  $\tau$  (s) represents the restore constant of one day and  $C_3$  represents the dimensionless force–restore coefficient for the total soil column.

#### e. Routing to the outlet

The output water fluxes of ISBA—that is, total runoff and deep drainage—are routed at the same time step as the lateral water distribution performed within TOPMODEL (one hour for this study). When an ISBA mesh is partially covered or not covered by a TOPMODEL catchment, the original equations of ISBA apply on the partial or total mesh not simulated by TOPMODEL. The contribution to the runoff and deep drainage produced by the original ISBA formulation are not routed. The deep drainage and the subsurface runoff are distributed uniformly over the TOPMODEL pixels within the ISBA mesh, whereas the surface runoff is distributed only over the saturated TOPMODEL pixels.

The total runoff and deep drainage are routed to the outlet using a geomorphological method. For each

TOPMODEL pixel, this method specifies the time needed for the water to reach the outlet. It uses the channel network determined from the DEM. For the total runoff, a constant velocity  $V_h$  is applied to route it on the hillslope to the hydrographic network and then a constant velocity  $V_r$  in the river to reach the outlet of the catchment. A constant velocity  $V_g$  within the ground for the drainage is also considered, to route it to the hydrographic network. The hillslope velocity  $V_h$  is generally one order lower than the velocity in the river  $V_r$  (Zin and Obled 2009, manuscript submitted to *J. Hydrol.*). In the context of Mediterranean flash floods, the drainage flux is not the main production process of the flash flood. Consequently, the velocity within the ground is not a sensitive parameter. Thus, a constant speed of  $0.3 \text{ m s}^{-1}$  was used. Concerning the hillslope and river velocities, we respected the following equation:

$$V_r = 10V_h. \quad (\text{A14})$$

Some sensitivity tests were carried out with hillslope speeds (and associated river speeds) of 0.1, 0.2 and  $0.3 \text{ m s}^{-1}$ . These sensitivity tests led to the values for  $V_h$  and  $V_r$  of 0.1 and  $1 \text{ m s}^{-1}$ , respectively, used in this study.

#### REFERENCES

- Beven, K. J., 1982: On subsurface stormflow: An analysis of response times. *Hydrol. Sci. J.*, **27**, 505–521.
- , and M. J. Kirkby, 1979: A physically based variable contributing area model of basin hydrology. *Hydrol. Sci. Bull.*, **24**, 43–69.
- , R. Lamb, R. Romanowicz, and J. Freer, 1995: TOPMODEL. *Computer Models of Watershed Hydrology*, V. P. Singh, Ed., Water Resources Publications, 627–668.
- Bonnifant, L., G. Delrieu, M. Le Lay, B. Boudevillain, A. Masson, P. Belleudy, E. Gaume, and G. M. Saulnier, 2009: Hydrologic and hydraulic distributed modeling with radar rainfall input: Reconstruction of the 8–9 September 2002 catastrophic flood event in the Gard region, France. *Adv. Water Resour.*, **32**, 1077–1089.
- Boone, A., V. Masson, T. Meyers, and J. Noilhan, 2000: The influence of the inclusion of soil freezing on simulations by a soil–vegetation–atmosphere transfer scheme. *J. Appl. Meteor.*, **39**, 1544–1569.
- Bubnová, R., A. Horányi, and S. Malardel, 1993: International project ARPEGE/ALADIN. *EWGLAM Newsletter*, No. 22, Institut Royal Météorologique de Belgique, Brussels, Belgium, 117–130.
- Cappus, P., 1960: Bassin expérimental d’Alrance—Étude des lois de l’écoulement—Application au calcul et à la prévision des débits (Alrance experimental watershed—Laws of flow study—Application to the calculation and the forecast of flows). *Houille Blanche*, **15A**, 493–520.
- Chen, J., and P. Kumar, 2001: Topographic influence on the seasonal and interannual variation of water and energy balance of basin in North America. *J. Climate*, **14**, 1989–2014.
- Clapp, R., and G. Hornberger, 1978: Empirical equations for some soil hydraulic properties. *Water Resour. Res.*, **14**, 601–604.

- Courtier, P., and J. F. Geleyn, 1988: A global numerical weather prediction model with variable resolution: Application to the shallow-water equation. *Quart. J. Roy. Meteor. Soc.*, **114**, 1321–1346.
- Deardorff, J. W., 1977: A parameterization of ground-surface moisture content for use in atmosphere prediction models. *J. Appl. Meteor.*, **16**, 1182–1185.
- Decharme, B., and H. Douville, 2006: Introduction of a sub-grid hydrology in the ISBA land surface model. *Climate Dyn.*, **26**, 65–78.
- , —, A. Boone, F. Habets, and J. Noilhan, 2006: Impact of an exponential profile of saturated hydraulic conductivity within the ISBA LSM: Simulations over the Rhône basin. *J. Hydrometeorol.*, **7**, 61–80.
- Delrieu, G., and Coauthors, 2005: The catastrophic flash-flood event of 8–9 September 2002 in the Gard region, France: A first case study for the Cévennes–Vivarais Mediterranean Hydrometeorological Observatory. *J. Hydrometeorol.*, **6**, 34–52.
- Ducharne, A., R. D. Koster, M. J. Suarez, M. Stieglitz, and P. Kumar, 2000: A catchment-based approach to modelling land surface processes in a general circulation model. Part 2: Parameter estimation and model demonstration. *J. Geophys. Res.*, **105**, 24 823–24 838.
- Ducrocq, V., O. Nuisser, D. Ricard, C. Lebeaupin, and T. Thouvenin, 2008: A numerical study of three catastrophic precipitating events over southern France. Part II: Mesoscale triggering and stationarity factors. *Quart. J. Roy. Meteor. Soc.*, **134**, 131–145.
- Dümenil, L., and E. Todini, 1992: A rainfall-runoff scheme for use in the Hamburg climate model. *Adv. Theor. Hydrol.*, **9**, 129–157.
- Dune, T., and R. D. Black, 1970: Partial area contributions to storm runoff in a small New England watershed. *Water Resour. Res.*, **6**, 1296–1311.
- Famiglietti, J. S., and E. F. Wood, 1994: Multiscale modeling of spatially variable water and energy balance processes. *Water Resour. Res.*, **30**, 3061–3078.
- , —, M. Sivapalan, and D. J. Thongs, 1992: A catchment scale water balance model for FIFE. *J. Geophys. Res.*, **97**, 18 997–19 007.
- Gandin, L. S., 1963: *Objective Analysis of Meteorological Fields*. Gidrometeorologicheskoe izdat'stvo, 286 pp.
- Habets, F., and G. M. Saulnier, 2001: Subgrid runoff parameterization. *Phys. Chem. Earth*, **26**, 455–459.
- , and Coauthors, 1999: The ISBA surface scheme in a macroscale hydrological model applied to the Hapex-Mobilhy area. Part I: Model and database. *J. Hydrol.*, **217**, 75–96.
- , and Coauthors, 2008: The SAFRAN-ISBA-MODCOU hydrometeorological model applied over France. *J. Geophys. Res.*, **113**, D06113, doi:10.1029/2007JD008548.
- Huet, P., X. Martin, J.-L. Prime, P. Foin, C. Laurain, and P. Cannard, 2003: Retour d'expérience des crues de Septembre 2002 dans les départements du Gard, de l'Hérault, du Vaucluse, des Bouches du Rhône, de l'Ardèche et de la Drôme (Post-flood investigation of the September 2002 flood in the Gard, Hérault, Vaucluse, Bouches du Rhône, Ardèche and Drôme departments). Rapport de l'Inspection Générale de l'Environnement, Ministère de l'Ecologie et du Développement Durable, 133 pp. [Available online at [http://www.ecologie.gouv.fr/IMG/pdf/crues\\_gard.pdf](http://www.ecologie.gouv.fr/IMG/pdf/crues_gard.pdf).]
- Lafore, J. P., and Coauthors, 1998: The Meso-NH Atmospheric Simulation System. Part I: Adiabatic formulation and control simulations. *Ann. Geophys.*, **16**, 90–109.
- Lardet, P., and C. Obled, 1994: Real-time flood forecasting using a stochastic rainfall generator. *J. Hydrol.*, **162**, 391–408.
- Lebel, T., G. Bastin, C. Obled, and J.-D. Creutin, 1987: On the accuracy of areal rainfall estimation: A case study. *Water Resour. Res.*, **23**, 2123–2134.
- Le Lay, M., and G. M. Saulnier, 2007: Exploring the signature of climate and landscape spatial variabilities in flash flood events: Case of the 8–9 September 2002 Cévenne-Vivarais catastrophic event. *Geophys. Res. Lett.*, **34**, L13401, doi:10.1029/2007GLO29746.
- , —, S. Galle, L. Seguis, M. Metadier, and C. Peugeot, 2008: Model representation of the Sudanian hydrological processes: Application on the Donga catchment (Benin). *J. Hydrol.*, **363**, 32–41.
- Masson, V., J. L. Champeaux, F. Chauvin, C. Meriguet, and R. Lacaze, 2003: A global database of land surface parameters at 1-km resolution in meteorological and climate models. *J. Climate*, **16**, 1261–1282.
- Nash, J. E., and J. V. Stutcliffe, 1970: River flow forecasting through conceptual models part 1 – A discussion of principles. *J. Hydrol.*, **10**, 282–290.
- Niu, G. Y., and Z. L. Yang, 2003: The versatile integrator of surface atmospheric processes. Part II: Evaluation of three topography-based runoff schemes. *Global Planet. Change*, **38**, 191–208.
- Noilhan, J., and S. Planton, 1989: A simple parameterization of land surface processes for meteorological models. *Mon. Wea. Rev.*, **117**, 536–549.
- , and P. Lacarrere, 1995: GCM grid-scale evaporation from mesoscale modeling. *J. Climate*, **8**, 206–223.
- , and J. F. Mahfouf, 1996: The ISBA land surface parameterization scheme. *Global Planet. Change*, **13**, 145–159.
- Nuisser, O., V. Ducrocq, D. Ricard, C. Lebeaupin, and S. Anquetin, 2008: A numerical study of three catastrophic precipitating events over southern France. Part I: Numerical framework and synoptic ingredients. *Quart. J. Roy. Meteor. Soc.*, **134**, 111–130.
- Pellarin, T., G. Delrieu, G. M. Saulnier, H. Andrieu, B. Vignal, and J. D. Creutin, 2002: Hydrologic visibility of weather radar systems operating in mountainous regions: Case study for the Ardèche catchment (France). *J. Hydrometeorol.*, **3**, 539–555.
- Pellenq, J., 2002: Couplage de la modélisation hydrologique avec la modélisation des Transferts Sol-Végétation-Atmosphère: Application à la spatialisation et à l'assimilation des données du satellite SMOS (Coupling of hydrological modeling with Soil-Vegetation-Atmosphere Transfer modeling: Application to spatialization and assimilation of SMOS satellite data). Ph.D. thesis, University of Toulouse, 244 pp.
- , J. Kalma, G. Boulet, G. M. Saulnier, S. Wooldridge, Y. Kerr, and A. Chehbouni, 2003: A disaggregation scheme for soil moisture based on topography and soil depth. *J. Hydrol.*, **276**, 112–127.
- Quintana Seguí, P., and Coauthors, 2008a: Analysis of near-surface atmospheric variables: Validation of the SAFRAN analysis over France. *J. Appl. Meteor.*, **47**, 92–107.
- , E. Martin, F. Habets, and J. Noilhan, 2008b: Improvement, calibration and validation of a distributed hydrological model over France. *Hydrol. Earth Syst. Sci. Discuss.*, **5**, 1319–1370.
- Reed, S., V. Koren, M. Smith, Z. Zhang, F. Moreda, and D.-J. Seo, DMIP participants, 2004: Overall distributed model inter-comparison project results. *J. Hydrol.*, **298**, 27–60.
- Saulnier, G. M., and R. Datin, 2004: Analytical solving of a bias in the TOPMODEL framework water balance. *Hydrol. Processes*, **18**, 1195–1218.
- , C. Obled, and K. J. Beven, 1998: Including spatially variable effective soil depths in TOPMODEL. *J. Hydrol.*, **202**, 158–172.

- Seity, Y., P. Brousseau, S. Malardel, V. Masson, F. Bouttier, and G. Hello, 2008: Status of AROME developments. *ALADIN Newsletter*, No. 33, ALADIN Numerical Weather Prediction Project, Toulouse, France, 40–47.
- Stieglitz, M., D. Rind, J. Famiglietti, and C. Rosenzweig, 1997: An efficient approach to modeling the topographic control of surface hydrology for regional and global climate modeling. *J. Climate*, **10**, 118–137.
- Taha, A., J. M. Gresillon, and B. E. Clothier, 1997: Modelling the link between hillslope water movement and stream flow: Application to a small Mediterranean forest watershed. *J. Hydrol.*, **203**, 11–20.
- Vincendon, B., and Coauthors, 2008: Flash flood forecasting within the PREVIEW project: Value of high-resolution hydrometeorological coupled forecast. *Meteor. Atmos. Phys.*, **103**, 115–125.
- Wood, E., D. Lettenmaier, and V. Zartarian, 1992: A land-surface hydrology parameterization with subgrid variability for general circulation models. *J. Geophys. Res.*, **97**, 2717–2728.
- Zehe, E., R. Becker, A. Bárdossy, and E. Plate, 2005: Uncertainty of simulated catchment runoff response in the presence of threshold processes: Role of initial soil moisture and precipitation. *J. Hydrol.*, **315**, 183–202.